Metabolic trait means but not correlations differ among fungal endophytes isolated from the same plant species

Emile Gluck-Thaler[1,2*], Muhammad Shaikh[1], Corlett W. Wood[1]

(1) Department of Biology, University of Pennsylvania, Philadelphia, USA
(2) Current address: Laboratory of Evolutionary Genetics, University of Neuchâtel, Neuchâtel, Switzerland

*Corresponding author: emile.gluck@unine.ch

Summary

- Fungal endophytes are ubiquitous residents within plant tissues. While taxonomic characterization of endophyte communities is common, we know little about how even closely related individuals differ functionally because fungal taxonomy is often a poor predictor of variation in ecological traits, including those related to the metabolism of plant-derived substrates.
- Here, we tested whether two fungal endophyte lineages from the same family (Mollisiaceae) sampled from the same host species (*Vaccinium angustifolium*) differ phenotypically by comparing metabolic trait means and correlations related to growth across a panel of plant phenolics, carbohydrates, and tissue extracts.
- We found that lineages harbor significant, selectable metabolic variation. While one lineage grew faster across nearly all substrates, lineages differed in their mean response to specific substrates. For example, lineages responded differently to phenolics and carbohydrates, most dramatically for caffeic acid which abolished differences between lineages. However, most correlations between substrates within lineages were positive, suggesting that metabolic evolution is generally unconstrained by trade-offs among the examined traits.
- Our findings illustrate that characterizing multivariate phenotypes—measuring multiple metabolic traits and the correlations between them— provides key insight into the process of endophyte evolution and reveals that both fungal- and plant-specific determinants shape opportunities for ecological differentiation within plant microbiomes.

Key words: fungal endophyte, metabolism, trait architecture, multivariate phenotype, Mollisiaceae, *Vaccinium*, phenolic

Introduction

Organisms are composed of complex assemblages of traits and phenotypic correlations between these traits are ubiquitous (Lande & Arnold, 1983). Consequently, the evolution of any given trait depends not only on its direct effect on fitness, but also on the indirect effects of genetically correlated traits (Wagner, 2011). Characterizing variation in individual traits, as well as multivariate trait architectures (the strength and direction of trait correlations) is therefore essential for identifying evolutionary constraints, trade-offs and facilitations that together shape organismal adaptation (Opulente *et al.*, 2018). In contrast to macrobes where several decades of theoretical and empirical work have investigated evolutionary change through explicitly multivariate frameworks (Lande, 1979; Via, 1984; Ingleby *et al.*, 2014), we often lack a multivariate perspective on trait evolution in microbes such as bacteria and fungi (Obeng *et al.*, 2021). This lack of knowledge ultimately poses barriers for understanding both macrobial and microbial evolution because all plants and animals host diverse microbiomes of bacteria and fungi, and phenotypic variation expressed by microbial symbionts often has cascading ecological and evolutionary consequences for their hosts (McFall-Ngai *et al.*, 2013; Vandenkoornhuyse *et al.*, 2015).

Fungal endophytes - generally non-pathogenic fungi capable of colonizing living plant tissues - are major determinants of host phenotype (Saikkonen *et al.*, 2004; Ruotsalainen *et al.*, 2021). Their myriad activities influence outcomes at the organism, population, and ecosystem levels, often in an individual- or species-specific manner. For example, endophytic fungi shape the outcomes of plant interactions with pathogens (Busby *et al.*, 2013), mediate abiotic stress responses (Rodriguez *et al.*, 2008), promote or inhibit plant growth (Alberton *et al.*, 2010; Newsham, 2011; Reininger *et al.*, 2012) and structure plant communities (Aguilar-Trigueros & Rillig, 2016). Like many other fungal guilds, endophytes are distinct from animals and plants in that readily observable morphological traits, such as mycelial coloration and structure, are often poor indicators of ecological function (Koch et al. 2017; but see Aguilar-Trigueros *et al.*, 2022). Instead, many ecologically relevant traits in endophytes and other fungi at large are metabolic traits related to growth in the presence of particular substrates (Rokas *et al.*, 2018; Slot & Gluck-Thaler, 2019). As chemoheterotrophs, fungi must assimilate nutrients from organic matter to

grow. Furthermore, as sessile organisms incapable of escaping threats, fungi excel at degrading toxins that inhibit growth and synthesizing chemical deterrents that inhibit the growth of other organisms. Endophytic fungi spend much of their lives within plant tissues, and therefore must grow or at least survive within chemically complex environments consisting of mixtures of metabolites that serve different functions and whose activities impact each other (Gershenzon *et al.*, 2012). For example, many plants produce defense compounds like phenolics that inhibit fungal growth (Nicholson & Hammerschmidt, 1992; Westrick *et al.*, 2021), as well as carbohydrates that serve as carbon sources, promoting fungal growth (Hadacek & Kraus, 2002; Sun *et al.*, 2019). Determining how metabolic traits and trait architectures (i.e., growth rates and correlations between growth rates) differ among endophyte lineages thus stands to provide critical insight into endophyte ecology (Wisecaver *et al.*, 2014; Opulente *et al.*, 2018) and into their functioning in the context of their plant hosts.

High-throughput metabarcode sequencing has been extensively applied in recent years to characterize the phylogenetic diversity of plant-associated fungal communities (Nilsson *et al.*, 2019) and these data are often used as a proxy to characterize the functional diversity and ecological capacity of the examined communities (Zanne *et al.*, 2020). However, predicting microbial traits and phenotypes from phylogeny alone remains challenging because microbial phenotypes are often decoupled from their phylogenetic history such that even closely related lineages may not be ecologically similar (Boon *et al.*, 2014; Djemiel *et al.*, 2022). In particular, metabolic variation between fungal individuals may accumulate more rapidly than between other eukaryotes because fungi have relatively short generation times and acquire metabolic genes through horizontal transmission, which further complicate efforts to predict ecological differences based on relatedness alone (Wisecaver *et al.*, 2014). Additionally, mutations acquired during somatic growth are directly inherited by offspring because fungi do not have a dedicated germline. Consequently, we often lack robust expectations for how ecologically relevant metabolic traits vary among closely related fungi. Moreover, covariance in metabolic traits across suites of host-related metabolites are rarely measured (but see (Knapp & Kovács, 2016; LeBlanc *et al.*, 2017)), limiting our ability to predict how such traits will evolve within the complex biochemical environments of plant hosts.

Dark septate endophytes are a polyphyletic group of melanized Ascomycete fungi that dominate plant microbiomes across all major plant groups in terrestrial ecosystems (Ruotsalainen *et al.*, 2021). For example, the roots of *Vaccinium* species, a widely-distributed genus of shrubs that includes blueberry and cranberry, are frequently colonized by dark septate endophytes from the Molliciaceae family (Gorzelak *et al.*, 2012; Yang *et al.*, 2018; Morvan *et al.*, 2020). Individual Mollisiaceae endophytes often differ dramatically in their interactions with plants, ranging from commensal to mutualistic to pathogenic (Newsham, 2011; Tellenbach *et al.*, 2011; Reininger *et al.*, 2012), suggesting variation within and between species and lineages has important ecological consequences. Yet despite their potential to impact plant host function, our understanding of their phenotypic differences and of the ecological factors shaping their distributions is still in its infancy (Tanney & Seifert, 2020).

To gain insight into the evolutionary ecology of this important and widespread group of endophytes, we test the hypothesis that sister lineages of dark septate Mollisiaceae endophytes from the same host species differ in their metabolic phenotypes. We compared metabolic trait means and metabolic trait architectures within and between lineages, where we define a metabolic trait as growth on a particular plant-derived substrate. We first cultured two distinct lineages of Molliseaceae endophytes from the roots of lowbush blueberry (*Vaccinium angustifolium*) across three sites in Eastern North America. We then conducted two complementary experiments where we measured growth on media amended with one of eleven plant-produced carbohydrate and phenolic metabolites, or on media containing one of five tissue extracts from *Vaccinium* and other plant species (Figure 1A). The goal of the metabolite experiment was to reveal mechanistic insights into differences among lineages, while the goal of the plant tissue experiment was to phenotype endophyte growth in complex, ecologically realistic biochemical environments.

We ask two questions (Figure 1B): Do lineages differ in their mean response to plant metabolites and tissue extracts? And do lineages differ in their multivariate metabolic trait architecture, i.e., in the strength and orientation of trait correlations and in trade-offs in growth across metabolites or tissues? Given that certain fungi exhibit dominance-tolerance trade-offs between stress-associated traits and growth rate (Maynard *et al.*, 2019), and that specific phenolic compounds

and phenolic-rich plant tissues are likely sources of stress, we predicted that lineages would differ in their growth on phenolic and carbohydrate substrates, and in the strength and direction of trade-offs in growth across different metabolite and tissue substrates.

Materials and Methods

Endophyte and plant tissue collection

Lowbush blueberry (*V. angustifolium*) plants were sampled from June to October 2020 from three second growth forests in the Eastern United States that are primarily used for scientific research: the research forest at Chatham University's Eden Hall Campus in Richland Township, Pennsylvania (40°39'50.0" N 79°57'12.3" W); Powdermill Nature Reserve in Westmoreland County, Pennsylvania (40°09'41.1" N 79°16'28.9" W); and Mountain Lake Biological Station in Giles County, Virginia (37°22'34.2" N 80°31'12.1" W). At each location, we selected 2-7 sites located at least 500m apart, and within each site we haphazardly sampled 5-10 *V. angustifolium* individuals located at least 10m apart with no observable blueberry plants between them. Fine fibrous roots located no deeper than 10cm from the soil surface were collected from individual plants using a trowel and knife, stored in plastic bags, and used immediately that same day for endophyte isolation.

At Mountain Lake Biological Station in October 2020, we collected additional plant tissues to use in the preparation of growth media for two experiments (see below). Whole root systems and attached leaves from approximately 50 *V. angustifolium* plants growing from three large patches were collected on a single day. Root systems and leaves were pooled across sample sites. We also haphazardly collected fallen leaves from *Quercus* spp. (oak) and *Acer* spp. (maple), and fallen needles from a stand of planted *Pinus monticola* (western white pine). All roots and leaves were kept at -80°C for approximately four months until used for media preparation.

Endophyte isolation and genotyping

Endophytic fungi were isolated from *V. angustifolium* roots using a sequence of ethanol/bleach sterilization steps followed by direct plating onto 50% strength Modified Melin-Norkrans agar (MMN; Supporting information Methods S1). A total of 69 fungi isolated from *V. angustifolium* roots with melanized morphologies characteristic of dark septate endophytes were successfully genotyped by sequencing the internal transcribed spacer (ITS) barcoding gene (Table S1)(Gardes

and Bruns 1993). We identified each isolate to taxonomic family level using a BLASTn search of their ITS sequence against the NCBI nr/nt database (last accessed 01/31/2021). The resulting sample of ITS sequences from Mollisiaceae isolates, along with reference sequences from known species within this family (Tanney & Seifert, 2020), were aligned using mafft (--auto)(Katoh & Standley, 2013). Alignments were trimmed using ClipKit (default settings)(Steenwyk *et al.*, 2020), and used to build a maximum likelihood phylogeny with IQtree (-m MFP -b 100)(Nguyen *et al.*, 2015). This phylogeny revealed that 52 isolates could be confidently placed within the Mollisiaceae family.

Given that species-level classifications are notoriously difficult to resolve in the Mollisiaceae, we used the phylogenetic placements of our isolates relative to the closest described species to provisionally classify them into one of two lineages: the *Phialocephala fortinii* s.l. – *Acephala applanata* species complex (PAC) and "Clade D" (Tanney and Seifert 2020). PAC contains some of the most well-studied and frequently recovered dark septate endophyte species from coniferous and ericaceous plant roots (Grünig et al. 2008). Clade D is an ad-hoc phylogenetic group which includes *Mollisia nigrescens* and other poorly described root endophytes that have previously been recovered from *Vaccinium* tissues (Tanney and Seifert 2020).

We initially selected 17 isolates from each lineage to phenotype by prioritizing isolates with different ITS sequences and/or that were recovered from different host individuals (Figure 2). We ultimately filtered out several isolates due to quality control issues, resulting in 13 Clade D isolates and 17 PAC isolates (Supporting information Methods S1)(Parks & Goldman, 2014). While both Clade D and PAC isolates were recovered from the Mountain Lake site ($n_{\text{Clade D}}$ = 10; n_{PAC} = 14), only Clade D isolates were retained from the Chatham site ($n_{\text{Clade D}}$ = 3) and only PAC isolates were retained from the Powdermill site (n_{PAC} = 3).

Plant metabolite experiment: media preparation and experimental design

We selected 6 phenolic and 5 carbohydrate metabolites produced across different tissues in *Vaccinium* and therefore likely encountered by fungal endophytes colonizing species within this genus (Table S2). We added each metabolite to media amended with a hot water extraction of *V. angustifolium* root tissue (Supporting information Methods S1). Each of the 11 treatments

consisted of known physiological concentrations of each metabolite (Stribley & Read, 1974; Harris *et al.*, 2007; Riihinen *et al.*, 2008; Kaur *et al.*, 2012; Edwards *et al.*, 2018; Ștefănescu *et al.*, 2020). We used media amended with host root tissue to capture the effect that each metabolite may have on endophyte growth in the context of other host-associated metabolites, as opposed to adding metabolites to standardized minimal media. As a control treatment, we added 20ml of pure ethanol to root extract media (ethanol was used to dissolve all metabolite treatments), for a total of 12 treatments.

We ran this experiment in three cohorts separated by 1-2 weeks each. Each cohort had one replicate of each isolate-metabolite combination (34 isolates x 12 treatments = 408 plates / cohort). All plates for a given cohort were prepared on the same day using root tissue from one of the six original bags of *V. angustifolium* root system collections (see above) and left to dry for 48 hours in a laminar flow hood. Plates were then inoculated with 4mm plugs from two-week old cultures grown on MMN plates, sealed with micropore tape, haphazardly arranged and incubated upside-down in the dark at room temperature.

Plant tissue experiment: media preparation and experimental design

We selected root and leaf tissues from *V. angustifolium,* as well as leaves from three different plant species sympatric with *V. angustifolium* (*Pinus monticola*, *Quercus* spp. and *Acer* spp.). We used these additional plant species to create ecologically relevant variation in multivariate biochemical environments for the plant tissue experiment. We prepared root and leaf extracts from materials collected at Mountain Lake Biological Station (see above) using a hot water extraction method (Supporting information Methods S1).

Autoclaved extracts were added to autoclaved DI water agar (15g/L) to a final concentration of 5g/L, and the resulting solutions were immediately poured into plates prepared and left to dry as above. Final tissue extract concentrations in this experiment were 5 times greater than those in the metabolite experiment because they were intended as the main treatment effect. There were 3 replicates per isolate x tissue treatment (34 isolates x 5 treatments x 3 replicates = 510 plates), and a single experimental cohort. All plates were prepared on the same day and inoculated and stored as above.

Data collection

Given that many Mollisiaceae endophytes primarily reproduce through clonal vegetative growth (Tanney & Seifert, 2020), growth rates are expected to be important ecological traits (Aguilar-Trigueros *et al.*, 2015). We measured colony area in cm^2 at 7, 14, and 21 days after inoculation and calculated the Area Under the Growth Progress Stairs (AUGPS) as a quantitative measurement of growth over time, such that AUGPS units were cm^2 x 7 days (Supporting information Methods S1). We calculated AUGPS using the audps function (type = "absolute") in the R package Agricolae (Mendiburu and Simon 2015). All plates whose isolates did not grow over the 21-day period were discarded.

Haphazardly selected groups of plates were imaged using a vertically mounted Nikon D3500 camera equipped with a Nikon AF-P DX 18-55mm f/3.5-5.6G VR lens. A ruler was placed in each image and was used to calibrate measurements. Plates were illuminated from two sides by mounted fluorescent lights. We measured colony area from images of each plate using ImageJ software (Schneider *et al.*, 2012), where the boundaries of each colony were estimated by eye. The colony area at day 0 for all isolates (0.113 cm^2) was determined based on a random sample of 10 plates imaged at this time. Colonies without identifiable boundaries were marked as missing. Images from the tissue experiment taken on day 21 were discarded because the media progressively darkened over this period of time such that the fungal colony boundaries could not reliably be identified.

Statistical analysis: Linear mixed models

Prior to our analyses, we removed 4 isolates originally assigned to Clade D from our dataset due to poor phylogenetic support (Supporting information Methods S1). In addition, we removed 4 isolates (2 PAC and 2 Clade D) from the metabolite experiment and 1 PAC isolate from the tissue experiment due to possible contamination (Supporting information Methods S1). We performed all statistical analyses in R 4.1.1 (R Core Team 2016) and unless specified otherwise, created data visualizations using ggplot2 (Wickham et al. 2021). We constructed three different linear mixed models to test for the effects of various predictor variables on isolate growth (i.e., AUGPS) using the "lmer" function in the lme4 package (Bates et al. 2015). We included isolate

and isolate-by-treatment interactions as random effects in all models to control for isolate-specific variation.

To test how individual metabolites affected isolate growth in the two endophyte lineages, we constructed a model with metabolite, phylogenetic lineage, metabolite-by-lineage interactions and cohort as fixed effects. To test how chemical class (phenolic or carbohydrate) interacts with lineage membership, we constructed a model with chemical class, phylogenetic lineage, class-by-lineage interactions and cohort as fixed effects and individual metabolite as a random effect to control for metabolite-specific effects independent of chemical class. Finally, to test how plant tissues interact with lineage membership, we constructed a model that included tissue, phylogenetic lineage and replicate as fixed effects.

We tested for the significance of fixed effects with type III sums of squares using the Anova function in the car package (Fox and Weisberg 2011). We confirmed that the residuals within each model met the required assumptions of normality and homoscedasticity by simulating model residuals using the DHARMa package (Hartig and Lohse 2021) and inspecting the resulting quantile-quantile plot and the plot of the residuals versus the predicted values to detect deviations from the expected distribution. Estimated marginal means and their 95% confidence intervals for each treatment within each lineage were calculated and compared to each other using the emmeans package and post-hoc Tukey tests (Lenth et al. 2021).

Statistical analysis: Comparisons and visualization of multivariate phenotype matrices

To test for differences in the multivariate response to plant chemistry between the two lineages, we compared the phenotypic variance/covariance (**P**) matrices from each lineage for the plant metabolite and plant tissue experiments, in addition to carbohydrate- and phenolic-specific **P** matrices. In these **P** matrices, each trait is growth (AUGPS) on a different metabolite or plant tissue. In order to avoid artificially inflating similarity between **P** matrices, we removed metabolite treatments from the metabolite experiment that had no statistically significant effect on growth in either lineage (Table S3). This resulted in the removal of two phenolic treatments (chlorogenic acid and vanillic acid) and one carbohydrate treatment (starch). Removal of these treatments do not quantitatively change the results of any multivariate statistical analyses (data not shown). For the metabolite experiment, we averaged growth across cohorts (which were

equivalent to experimental replicates) and for the tissue experiment, we averaged across replicates. We decomposed each **P** matrix into its eigenvectors and eigenvalues using base R's prcomp function.

We calculated three test statistics that capture differences in matrix structure (Figure 1), following previously established methods (Wood and Brodie III 2015): the difference in total metabolic trait variance between endophyte lineages (ΔVt), the difference between the proportion of variance along P_{max} (ΔP_{max}), and the difference in the orientation of P_{max} (θ). P_{max} represents the largest eigenvector of the covariance matrix and is the linear combination of traits that captures the largest proportion of variation in growth among isolates. A large ΔVt indicates that isolates within one lineage vary more than do isolates in the other lineage. A large ΔP_{max} indicates that growth on different substrates is more strongly correlated in one lineage than in the other. A large θ indicates that the lineages differ in the direction of trait correlations. To test whether ΔVt, ΔP_{max}, or θ differed between lineages, we permuted isolates among the two lineage matrices 500 times and recalculated the three test statistics as above from the permuted data to generate null distributions.

To quantify similarity in overall matrix structure, we calculated correlations between the response to random vectors applied to each lineage's **P** matrix using the RandomSkewers function from the evolqg package with 10,000 random gradients (Melo et al. 2016). The random skewers (RS) method applies random vectors of selection gradients to each matrix and measures the correlation between the response vectors of the two matrices. The responses of matrices with similar structures will be highly correlated. To examine pairwise correlations between growth on different substrates, we constructed Spearman correlation matrices using base R's cor function. The significance of each correlation coefficient was visualized and calculated using the ggcorplot package (Kassambara 2019). Pairwise trait correlations between lineages were compared using the cocor package using the Fisher's z test (Diedenhofen & Musch, 2015). *P* values were corrected for multiple comparisons using the Benjamini-Hochberg method implemented in base R's p.adjust function.

Results

Lineages differ in baseline growth rates and in their growth on individual plant metabolites, chemical classes and tissues

For the plant metabolite experiment, we found that lineages differed in their baseline growth (lineage effect: $\chi^2_{df=1} = 175.43$, $P < 0.0001$), that metabolites differed in their effects on growth (metabolite effect: $\chi^2_{df=11} = 238.75$, $P < 0.0001$), and that lineages differed in their growth on individual metabolites (lineage-by-metabolite interaction: $\chi^2_{df=11} = 345.16$, $P < 0.0001$)(Figure 3; Table S4). The mean growth of the PAC isolates averaged across all treatments and cohorts was significantly greater than the growth of Clade D isolates (LS means: PAC = 64.4 cm^2 x 7 days, Clade D = 31.3 cm^2 x 7 days; $P < 0.0001$). In Clade D, growth on rutin, caffeic acid and xylose all differed significantly from the ethanol control media, while in the PAC, all metabolite treatments except chlorogenic acid, vanillic acid and starch differed significantly from the control (Table S5, Figure 3). Treatments with significant effects tended to increase growth, except caffeic acid which negatively affected the PAC (Table S6). The positive effect of caffeic acid on Clade D was such that growth rate differences between the two lineages were abolished when growing on this metabolite after correcting for multiple comparisons (LS means: PAC = 50.7 cm^2 x 7 days, Clade D = 42.9 cm^2 x 7 days; $P_{Bonferroni} = 0.234$). We additionally found a significant effect of experimental cohort ($\chi^2_{df=2} = 126.92$, $P < 0.0001$), indicating that growth rates differed between our experimental cohorts. Differences between treatments were not due to total carbon concentration, as carbon molarity was not significantly correlated with growth in either lineage across all treatments (Pearson's $r_{PAC} = 0.01$, $P_{PAC} = 0.83$; Pearson's $r_{Clade\ D} = 0.02$, $P_{Clade\ D} = 0.68$; Figure S1).

We classified all 11 metabolites into two chemical classes: carbohydrates and phenolics. We found that lineages differed in their baseline growth across both chemical classes (lineage effect: $\chi^2_{df=1} = 183.38$, $P < 0.0001$) and that lineages differed in their growth on individual chemical classes (lineage by chemical class interaction: $\chi^2_{df=1} = 74.50$, $P < 0.0001$). However, phenolics and carbohydrates alone did not differ in their impact on endophyte growth (chemical effect: $\chi^2_{df=1} = 0.35$, $P = 0.55$; Table S7). These main effects were still significant when excluding the caffeic acid treatment (Table S8). The mean growth of PAC isolates was

significantly greater than Clade D isolates on both chemical classes (Table S9); however, the magnitude of difference was greater on carbohydrates than on phenolics (LS means for carbohydrates: PAC = 67.7 cm^2 x 7 days, Clade D = 27.8 cm^2 x 7 days; LS means for phenolics: PAC = 61.2 cm^2 x 7 days, Clade D = 33.8 cm^2 x 7 days), and remained true when excluding caffeic acid treatments (Table S10). We also found a significant effect of experimental cohort (cohort effect: $\chi^2_{df=2} = 32.48$, $P < 0.0001$), indicating once again that growth rates differed between cohorts.

For the plant tissue experiment, we similarly found that lineages differed in their baseline growth (lineage effect: $\chi^2_{df=1} = 542.31$, $P < 0.0001$), that tissue extracts differed in their effect on growth (tissue effect: $\chi^2_{df=4} = 394.12$, $P < 0.0001$), and that lineages responded differently to individual plant tissues (lineage by tissue effect: $\chi^2_{df=4} = 205.92$, $P < 0.0001$)(Table S11, Figure 3). The mean growth of PAC isolates was significantly greater than that of Clade D isolates averaged across all tissue types (LS means: PAC = 33.1 cm^2 x 7 days, Clade D = 11 cm^2 x 7 days; $P < 0.0001$). Within the PAC, growth on the oak and maple leaf extracts was significantly greater compared with growth on all other extracts, while within Clade D, only the oak leaf treatment was significantly greater compared with all other treatments (Table S12).

The majority of variation within each lineage arises from differences between fast and slow growing isolates

For the metabolite experiment, the major principal component of the phenotypic variance-covariance (**P**) matrix (PC1, or P_{max}) captured 59.1% of variation in growth rate across treatments for PAC and 74.8% for Clade D (Figure 4). All metabolite treatments had similar loadings on P_{max} within each lineage, suggesting this axis separates isolates according to how fast or slow they grow independent of any specific treatment. In contrast, treatments differ in their loadings on the second principal component (PC2), which suggests that this axis instead separates isolates according to metabolite-specific growth responses. Across lineages, the loadings of the metabolite treatments on P_{max} are strongly correlated with each other (Pearson's $r_{df=7} = 0.73$, $P = 0.03$). This indicates that P_{max} from either lineage are largely similar to each other and thus directly comparable (Figure 4). Conversely, the loadings on PC2 within each

lineage are not correlated (Pearson's $r_{df=7}$ = -0.37, P = 0.33), indicating that they capture lineage-specific responses to treatments.

For the plant tissue experiment, P_{max} captured 70% of variation in growth rate for PAC and 71% for Clade D. The loadings of the tissue treatments on P_{max} from different lineages were not significantly correlated with each other (Pearson's $r_{df=3}$ = -0.67, P = 0.221), suggesting that P_{max} captures different aspects of each lineage's multivariate response to plant tissues.

Metabolic traits vary with similar strength and in similar directions along the major axis of multivariate growth

The total phenotypic variance of PAC was nearly twice the magnitude of Clade D (200 vs. 110), indicating that there was more variation in growth across metabolites in PAC isolates than Clade D isolates. The difference in total phenotypic variance (ΔVt) between the two lineages for the metabolite experiment was significantly greater than expected compared to random chance (P = 0.02; Figure 4). Lineages differed marginally in the proportion of variation explained by P_{max} (ΔP_{max}) compared with random expectations (P = 0.09), indicating that the strength with which traits covary along P_{max} is largely similar among isolates from either lineage. Finally, the difference in the orientation of P_{max} (θ) was smaller than expected (P = 0.05), indicating that within each lineage, the directions in which traits covary are conserved along P_{max}.

The comparisons of P_{max} for the metabolite experiment, which provide comparisons along a single dimension of the **P** matrix, are in agreement with comparisons of overall **P** matrix structure. Random skewers showed that the response to selection predicted from the **P** matrices for the two lineages was strongly correlated (random skewers correlation = 0.88, P <0.001). This correlation is not likely not driven by a response to a specific chemical class, as the carbohydrate-specific and phenolic-specific **P** matrices were also significantly correlated across the two lineages (random skewers $\text{correlation}_{carbohydrates}$ = 0.96, P = 0.005; random skewers $\text{correlation}_{phenolics}$ = 0.88, P = 0.025). This indicates that overall, traits vary with similar strength and in similar directions across all dimensions of the **P** matrix.

In contrast for the tissue experiment, differences between lineages in total phenotypic variance (ΔVt; P = 0.609), the proportion of variation on P_{max} (ΔP_{max}; P = 0.431) and the orientation of P_{max} (θ; P = 0.719) did not differ more or less compared to a random expectation.

This indicates that PAC isolates are about as different from each other as Clade D isolates when growing on plant tissues and that their traits vary with similar strength and in similar directions (Figure 4). Similar to the metabolite experiment, a random skewers analysis showed that the **P** matrices of the two lineages were positively correlated with each other (Random skewers correlation = 0.82, P = 0.026).

The strength and direction of pairwise metabolic trait correlations are conserved

After comparing the overall multivariate responses of the two lineages, we next compared all pairwise trait correlations between the two lineages to test whether any substrate-specific differences in metabolic trait architecture exist. For the metabolite experiment, all trait correlations tended to be positive within each lineage, with 36/36 showing positive trends in both lineages and with 16/36 of these having positive correlations significantly greater than 0 in both lineages (Figure S2). For the tissue experiment, all pairwise trait correlations within each lineage were positive, and 4/10 correlations were significantly greater than 0 in both lineages (Figure S2). After correcting for multiple comparisons, we found no evidence that pairwise trait correlations differed between lineages for the metabolite experiment, while only the oak leaf-pine needle trait correlation differed between lineages for the tissue experiment (Spearman's $rho_{Clade\ D}$= 0.9, Spearman's rho_{PAC}= 0.2; Fisher's z = -3.01; P = 0.03; Table S13, Figure 5).

Discussion

It has been historically challenging to translate measurements of microbial phylogenetic diversity into predictions of functional diversity (Rodriguez *et al.*, 2009; Djemiel *et al.*, 2022) because phenotypic differences are difficult to predict from genetic sequence variation alone, especially among closely related individuals (Arnold & Lutzoni, 2007; Grünig *et al.*, 2008; Johnson *et al.*, 2012; Hazard *et al.*, 2017; U'Ren *et al.*, 2019; Harrison & Griffin, 2020; Liber *et al.*, 2022). To address this major gap, we compared the multivariate metabolic phenotypes of sister lineages of fungal endophytes and found that lineages harbor significant and selectable phenotypic variation related to growth on plant-derived metabolites and tissues. Our metabolite experiment showed that lineages differ primarily in mean growth rate, and our tissue experiment showed that these differences persisted across the complex biochemical environments of plant tissue extracts (Figure 3), suggesting intrinsic fungal growth rates provide a major opportunity for metabolic niche differentiation. However, while differences in mean growth rate accounted for the majority of variation between lineages, we found that lineages responded differently to plant carbohydrates and phenolics overall as well as to specific metabolites like caffeic acid, indicating that lineage-specific responses to plant metabolites have evolved. In contrast to our expectation that trait correlations would differ between lineages, multivariate trait relationships across plant metabolites and tissues are broadly conserved between lineages (Figure 4, Figure 5). We found no evidence of trade-offs in either lineage between any substrates, suggesting the evolution of the metabolic traits we examined here is generally unconstrained. Our findings add to the growing realization that even closely related lineages may differ in key aspects of their preferred ecological niche (Louca, Parfrey, and Doebeli 2016) and shed light on the nature of phenotypic variation among host-associated microbes.

Growth rate variation provides a primary opportunity for metabolic differentiation

Although closely-related organisms are typically assumed to be ecologically similar, the sister lineages of Molliseaceae endophytes in our experiment differed in baseline growth rates across nearly all examined metabolites and tissues, and these differences account for the majority of phenotypic variation between lineages (Figure 3). Differences in growth rate accounted for the

majority of phenotypic variation within each lineage as well, such that fast growers are typically fast and slow growers are typically slow across all examined substrates (Figure 4). Contrary to our initial expectations, we did not detect trade-offs between growth on different substrates within either lineage (Figure 5, Figure S2). The differences between lineages in intrinsic growth persisted across the plant tissue extracts, indicating that lineages also differ in growth rate in more complex, ecologically realistic metabolic environments.These findings are further reflected in the fact that neither the orientation nor magnitude of the major axis of phenotypic variation P_{max} differs between lineages for either metabolite- or tissue-related growth phenotypes (Figure 4). Together, the conservation of pairwise positive trait correlations and the major axis of multivariate trait variation suggests that these closely-related lineages have maintained a common metabolic trait architecture after diverging from a common ancestor.

Many fungi display dominance-tolerance trade-offs where isolates diverge along a continuum of stress-tolerant and slow-growing to stress-sensitive and fast-growing (Maynard *et al.*, 2019; Lustenhouwer *et al.*, 2020). For this reason, we initially predicted that we would observe a trade-off between growth on substrates that induce stress (phenolics) and those that typically do not (carbohydrates). To our surprise, although lineages responded differently to phenolics and carbohydrates (Figure 3), we did not observe any broad trade-offs between growth on these different substrates. Future studies should examine alternative ecological traits beyond those directly related to plant metabolites, such as abiotic stress tolerance and combative dominance, in order to test whether differences in intrinsic growth rates reflect trade-offs with other traits (Bazzaz & Grace, 1997; Crowther *et al.*, 2014; Zanne *et al.*, 2020).

Plant metabolites and tissues also shape opportunities for metabolic differentiation

Lineages responded in a broadly similar way to specific plant metabolites and tissues (Figure 3). A notable exception was caffeic acid, which decreased growth in the PAC lineage and increased growth in the Clade D lineage such that growth rates among lineages are abolished in the presence of this metabolite. Caffeic acid is a common metabolite produced by many plants as a precursor in the production of lignin and is also known to directly inhibit the growth of several bacteria and fungi (Ravn *et al.*, 1989), suggesting it has potential to act as a defense compound both through strengthening plant cell walls and inhibiting microbial colonization of plant tissues.

In tobacco, bacterial pathogens induce caffeic acid secretion in root exudates (Li *et al.*, 2021), and fungal colonization of barley plants induces the secretion of fungitoxic biochemical derivatives of caffeic acid (Lanoue *et al.*, 2010).

The lineage-specific effects we observed for substrates like caffeic acid may arise through several non-mutually exclusive mechanisms. A lineage that responds neutrally to a substrate with a negative effect in another lineage may produce enzymes that detoxify or assimilate the substrate and free isolates from its suppressive effects, or may have other compensatory mechanisms for tolerating downstream stresses such as reactive oxygen species that often result from toxin activity (Westrick *et al.*, 2021). Additionally, lineages with a positive response to an otherwise neutral substrate may either simply possess the requisite metabolic enzymes for its assimilation or may have enzymes that more effectively catalyze its assimilation. In the case of caffeic acid, Clade D's increase in growth coupled with PAC's decrease in growth suggests that Clade D isolates are able to use what is otherwise a toxic compound as a carbon source (Figure 3). Indeed, Clade D tends to have higher growth across all examined phenolics compared to all carbohydrates, while the opposite is true for PAC. This suggests that Clade D in general is better equipped to assimilate phenolic compounds and PAC is better equipped to assimilate carbohydrates such that phenolics tend to decrease differences in growth rate between lineages.

Our direct characterization of metabolic traits related to plant metabolites and tissues adds a fungal-based perspective to the growing body of knowledge highlighting the potential of plant chemistry to act as a deterministic filter shaping endophyte community composition through differentially impacting endophyte growth (Bailey *et al.*, 2005; Saunders & Kohn, 2009; González-Teuber *et al.*, 2020; Christian *et al.*, 2020). Multitudes of fungi often colonize the same plant host species (Arnold & Lutzoni, 2007; U'Ren *et al.*, 2019; Harrison & Griffin, 2020), raising the question of just how much they differ in their ecological and metabolic niches. We show that even closely related lineages of endophytic fungi differ in intrinsic growth rates, and in their response to several plant-derived metabolites, metabolite types and plant tissues. Our results suggest that these differences evolve over relatively short evolutionary timescales, and caution against assuming that closely related endophyte lineages are ecologically redundant. Differences in growth rates and in the ability to grow on specific plant metabolites and tissues may have cascading ecological consequences, favouring the assembly of distinct fungal communities

associated with particular host species and genotypes (Sietiö *et al.*, 2018; Bonito *et al.*, 2019) and likely shaping the distribution of fungal populations across landscapes (Tedersoo et al. 2013; Wehner et al. 2014; Veach et al. 2019). Further investigations of phenotypic variation among endophytes will be important for dissecting their impacts on plant health and ecosystem function and for predicting how microbiomes will respond to environmental disturbance (Moran, Hartig, and Bell 2016).

Acknowledgements

We are grateful for the help of Marion Holmes and Tiffany Betras for getting us to and from our sample sites and providing expert guidance. Thanks to John Wenzel for providing access to the Powdermill Nature Reserve, Jaime Jones for facilitating our sampling at Mountain Lake Biological Station and to McCall Calvert, Eunnuri Yi and Addison Martin for providing helpful feedback on the first draft of this manuscript. This work was supported by a Marie Skłodowska-Curie Individual Fellowship to EGT (proposal SEP-210615880-TRADEOFF) and startup funds from the University of Pennsylvania to CWW.

Contributions

EGT and CWW conceptualized the research. EGT and MS collected data and EGT conducted formal analyses. EGT wrote the original draft and EGT and CWW participated in reviewing and editing the manuscript.

Data availability

All supporting data, including raw image files, measurements and R scripts, are available from the following Figshare repository (DOI: 10.6084/m9.figshare.20489715). All sequence data have been deposited at NCBI (GenBank accession numbers OP378573 through OP378602).

Conflicts of interest

The authors declare that they have no conflicts of interests.

References

Aguilar-Trigueros CA, Boddy L, Rillig MC, Fricker MD. **2022**. Network traits predict ecological strategies in fungi. *ISME Communications* **2**: 1–11.

Aguilar-Trigueros CA, Hempel S, Powell JR, Anderson IC, Antonovics J, Bergmann J, Cavagnaro TR, Chen B, Hart MM, Klironomos J, *et al.*2015. Branching out: Towards a trait-based understanding of fungal ecology. *Fungal Biology Reviews* **29**: 34–41.

Aguilar-Trigueros CA, Rillig MC. **2016**. Effect of different root endophytic fungi on plant community structure in experimental microcosms. *Ecology and Evolution* **6**: 8149–8158.

Alberton O, Kuyper TW, Summerbell RC. **2010**. Dark septate root endophytic fungi increase growth of Scots pine seedlings under elevated CO2 through enhanced nitrogen use efficiency. *Plant and Soil* **328**: 459–470.

Arnold AE, Lutzoni F. **2007**. Diversity and host range of foliar fungal endophytes: are tropical leaves biodiversity hotspots? *Ecology* **88**: 541–549.

Bailey JK, Deckert R, Schweitzer JA, Rehill BJ, Lindroth RL, Gehring C, Whitham TG. **2005**. Host plant genetics affect hidden ecological players: links among Populus, condensed tannins, and fungal endophyte infection. *Canadian Journal of Botany* **83**: 356–361.

Bazzaz FA, Grace J. **1997**. *Plant Resource Allocation*. Elsevier.

Bonito G, Benucci GMN, Hameed K, Weighill D, Jones P, Chen K-H, Jacobson D, Schadt C, Vilgalys R. **2019**. Fungal-Bacterial Networks in the Populus Rhizobiome Are Impacted by Soil Properties and Host Genotype. *Frontiers in Microbiology* **10**: 481.

Boon E, Meehan CJ, Whidden C, Wong DH-J, Langille MG, Beiko RG. **2014**. Interactions in the microbiome: communities of organisms and communities of genes. *Fems Microbiology Reviews* **38**: 90–118.

Busby PE, Zimmerman N, Weston DJ, Jawdy SS, Houbraken J, Newcombe G. **2013**. Leaf endophytes and Populus genotype affect severity of damage from the necrotrophic leaf pathogen, Drepanopeziza populi. *Ecosphere* **4**: art125.

Christian N, Sedio BE, Florez-Buitrago X, Ramírez-Camejo LA, Rojas EI, Mejía LC, Palmedo S, Rose A, Schroeder JW, Herre EA. **2020**. Host affinity of endophytic fungi and the potential for reciprocal interactions involving host secondary chemistry. *American Journal of Botany* **107**: 219–228.

Crowther TW, Maynard DS, Crowther TR, Peccia J, Smith JR, Bradford MA. **2014**.

Untangling the fungal niche: the trait-based approach. *Frontiers in Microbiology* **5**.

Diedenhofen B, Musch J. **2015**. cocor: A Comprehensive Solution for the Statistical Comparison of Correlations. *PLoS ONE* **10**: e0121945.

Djemiel C, Maron P-A, Terrat S, Dequiedt S, Cottin A, Ranjard L. **2022**. Inferring microbiota functions from taxonomic genes: a review. *GigaScience* **11**: giab090.

Edwards KR, Kaštovská E, Borovec J, Šantrůčková H, Picek T. **2018**. Species effects and seasonal trends on plant efflux quantity and quality in a spruce swamp forest. *Plant and Soil* **426**: 179–196.

Gershenzon J, Fontana A, Burow M, Wittstock U, Degenhardt J. **2012**. Mixtures of plant secondary metabolites: metabolic origins and ecological benefits. In: Iason GR, Dicke M, Hartley SE, eds. Ecological Reviews. The Ecology of Plant Secondary Metabolites: From Genes to Global Processes. Cambridge: Cambridge University Press, 56–77.

González-Teuber M, Vilo C, Guevara-Araya MJ, Salgado-Luarte C, Gianoli E. **2020**. Leaf resistance traits influence endophytic fungi colonization and community composition in a South American temperate rainforest. *Journal of Ecology* **108**: 1019–1029.

Gorzelak MA, Hambleton S, Massicotte HB. **2012**. Community structure of ericoid mycorrhizas and root-associated fungi of Vaccinium membranaceum across an elevation gradient in the Canadian Rocky Mountains. *Fungal Ecology* **5**: 36–45.

Grünig CRGR, Queloz VQ, Sieber TNSN, Holdenrieder OH. **2008**. Dark septate endophytes (DSE) of the Phialocephala fortinii s.l. – Acephala applanata species complex in tree roots: classification, population biology, and ecology. *Botany*.

Hadacek F, Kraus GF. **2002**. Plant root carbohydrates affect growth behaviour of endophytic microfungi. *FEMS microbiology ecology* **41**: 161–170.

Harris CS, Burt AJ, Saleem A, Le PM, Martineau LC, Haddad PS, Bennett SAL, Arnason JT. **2007**. A single HPLC-PAD-APCI/MS method for the quantitative comparison of phenolic compounds found in leaf, stem, root and fruit extracts of Vaccinium angustifolium. *Phytochemical Analysis* **18**: 161–169.

Harrison JG, Griffin EA. **2020**. The diversity and distribution of endophytes across biomes, plant phylogeny and host tissues: how far have we come and where do we go from here? *Environmental microbiology* **22**: 2107–2123.

Hazard C, Kruitbos L, Davidson H, Taylor AFS, Johnson D. **2017**. Contrasting effects of

intra- and interspecific identity and richness of ectomycorrhizal fungi on host plants, nutrient retention and multifunctionality. *New Phytologist* **213**: 852–863.

Ingleby FC, Hosken DJ, Flowers K, Hawkes MF, Lane SM, Rapkin J, House CM, Sharma MD, Hunt J. **2014**. Environmental heterogeneity, multivariate sexual selection and genetic constraints on cuticular hydrocarbons in Drosophila simulans. *Journal of Evolutionary Biology* **27**: 700–713.

Johnson D, Martin F, Cairney JWG, Anderson IC. **2012**. The importance of individuals: intraspecific diversity of mycorrhizal plants and fungi in ecosystems. *New Phytologist* **194**: 614–628.

Katoh K, Standley DM. **2013**. MAFFT Multiple Sequence Alignment Software Version 7: Improvements in Performance and Usability. *Molecular Biology and Evolution* **30**: 772–780.

Kaur J, Percival D, Hainstock LJ, Privé J-P. **2012**. Seasonal growth dynamics and carbon allocation of the wild blueberry plant (Vaccinium angustifolium Ait.). *Canadian Journal of Plant Science* **92**: 1145–1154.

Knapp DG, Kovács GM. **2016**. Interspecific metabolic diversity of root-colonizing endophytic fungi revealed by enzyme activity tests. *FEMS Microbiology Ecology* **92**.

Lande R. **1979**. Quantitative Genetic Analysis of Multivariate Evolution, Applied to Brain: Body Size Allometry. *Evolution* **33**: 402–416.

Lande R, Arnold SJ. **1983**. The Measurement of Selection on Correlated Characters. *Evolution* **37**: 1210–1226.

Lanoue A, Burlat V, Henkes GJ, Koch I, Schurr U, Röse USR. **2010**. De novo biosynthesis of defense root exudates in response to Fusarium attack in barley. *The New Phytologist* **185**: 577–588.

LeBlanc N, Essarioui A, Kinkel L, Kistler HC. **2017**. Phylogeny, plant species, and plant diversity influence carbon use phenotypes among Fusarium populations in the rhizosphere microbiome. *Phytobiomes Journal* **1**: 150–157.

Li S, Pi J, Zhu H, Yang L, Zhang X, Ding W. **2021**. Caffeic Acid in Tobacco Root Exudate Defends Tobacco Plants From Infection by Ralstonia solanacearum. *Frontiers in Plant Science* **12**.

Liber JA, Minier DH, Stouffer-Hopkins A, Van Wyk J, Longley R, Bonito G. **2022**. Maple and hickory leaf litter fungal communities reflect pre-senescent leaf communities. *PeerJ* **10**:

e12701.

Lustenhouwer N, Maynard DS, Bradford MA, Lindner DL, Oberle B, Zanne AE, Crowther TW. **2020**. A trait-based understanding of wood decomposition by fungi. *Proceedings of the National Academy of Sciences* **117**: 11551–11558.

Maynard DS, Bradford MA, Covey KR, Lindner D, Glaeser J, Talbert DA, Tinker PJ, Walker DM, Crowther TW. **2019**. Consistent trade-offs in fungal trait expression across broad spatial scales. *Nature Microbiology* **4**: 846–853.

McFall-Ngai M, Hadfield MG, Bosch TC, Carey HV, Domazet-Lošo T, Douglas AE, Dubilier N, Eberl G, Fukami T, Gilbert SF. **2013**. Animals in a bacterial world, a new imperative for the life sciences. *Proceedings of the National Academy of Sciences* **110**: 3229–3236.

Morvan S, Meglouli H, Lounès-Hadj Sahraoui A, Hijri M. **2020**. Into the wild blueberry (Vaccinium angustifolium) rhizosphere microbiota. *Environmental Microbiology* **22**: 3803–3822.

Newsham KK. **2011**. A meta-analysis of plant responses to dark septate root endophytes. *New Phytologist* **190**: 783–793.

Nguyen L-T, Schmidt HA, von Haeseler A, Minh BQ. **2015**. IQ-TREE: A Fast and Effective Stochastic Algorithm for Estimating Maximum-Likelihood Phylogenies. *Molecular Biology and Evolution* **32**: 268–274.

Nicholson RL, Hammerschmidt R. **1992**. Phenolic Compounds and Their Role in Disease Resistance. *Annual Review of Phytopathology* **30**: 369–389.

Nilsson RH, Anslan S, Bahram M, Wurzbacher C, Baldrian P, Tedersoo L. **2019**. Mycobiome diversity: high-throughput sequencing and identification of fungi. *Nature Reviews Microbiology* **17**: 95–109.

Obeng N, Bansept F, Sieber M, Traulsen A, Schulenburg H. **2021**. Evolution of Microbiota-Host Associations: The Microbe's Perspective. *Trends in Microbiology* **29**: 779–787.

Opulente DA, Rollinson EJ, Bernick-Roehr C, Hulfachor AB, Rokas A, Kurtzman CP, Hittinger CT. **2018**. Factors driving metabolic diversity in the budding yeast subphylum. *BMC Biology* **16**: 26.

Parks SL, Goldman N. **2014**. Maximum Likelihood Inference of Small Trees in the Presence of Long Branches. *Systematic Biology* **63**: 798–811.

Ravn H, Andary C, Kovács G, Mølgaard P. **1989**. Caffeic acid esters as in vitro inhibitors of plant pathogenic bacteria and fungi. *Biochemical Systematics and Ecology* **17**: 175–184.

Reininger V, Grünig CR, Sieber TN. **2012**. Host species and strain combination determine growth reduction of spruce and birch seedlings colonized by root-associated dark septate endophytes. *Environmental Microbiology* **14**: 1064–1076.

Riihinen K, Jaakola L, Kärenlampi S, Hohtola A. **2008**. Organ-specific distribution of phenolic compounds in bilberry (Vaccinium myrtillus) and 'northblue' blueberry (Vaccinium corymbosum x V. angustifolium). *Food Chemistry* **110**: 156–160.

Rodriguez RJ, Henson J, Van Volkenburgh E, Hoy M, Wright L, Beckwith F, Kim Y-O, Redman RS. **2008**. Stress tolerance in plants via habitat-adapted symbiosis. *The ISME journal* **2**: 404–416.

Rodriguez RJ, White Jr JF, Arnold AE, Redman RS. **2009**. Fungal endophytes: diversity and functional roles. *New Phytologist* **182**: 314–330.

Rokas A, Wisecaver JH, Lind AL. **2018**. The birth, evolution and death of metabolic gene clusters in fungi. *Nature Reviews Microbiology* **16**: 731–744.

Ruotsalainen AL, Kauppinen M, Wäli PR, Saikkonen K, Helander M, Tuomi J. **2021**. Dark septate endophytes: mutualism from by-products? *Trends in Plant Science* **0**.

Saikkonen K, Wäli P, Helander M, Faeth SH. **2004**. Evolution of endophyte–plant symbioses. *Trends in Plant Science* **9**: 275–280.

Saunders M, Kohn LM. **2009**. Evidence for alteration of fungal endophyte community assembly by host defense compounds. *The New Phytologist* **182**: 229–238.

Schneider CA, Rasband WS, Eliceiri KW. **2012**. NIH Image to ImageJ: 25 years of image analysis. *Nature Methods* **9**: 671–675.

Sietiö O-M, Tuomivirta T, Santalahti M, Kiheri H, Timonen S, Sun H, Fritze H, Heinonsalo J. **2018**. Ericoid plant species and Pinus sylvestris shape fungal communities in their roots and surrounding soil. *New Phytologist* **218**: 738–751.

Slot JC, Gluck-Thaler E. **2019**. Metabolic gene clusters, fungal diversity, and the generation of accessory functions. *Current Opinion in Genetics & Development* **58–59**: 17–24.

Steenwyk JL, Iii TJB, Li Y, Shen X-X, Rokas A. **2020**. ClipKIT: A multiple sequence alignment trimming software for accurate phylogenomic inference. *PLOS Biology* **18**: e3001007.

Ștefănescu B-E, Călinoiu LF, Ranga F, Fetea F, Mocan A, Vodnar DC, Crișan G. **2020**. The

Chemical and Biological Profiles of Leaves from Commercial Blueberry Varieties. *Plants* **9**: 1193.

Stribley DP, Read DJ. **1974**. The Biology of Mycorrhiza in the Ericaceae. *New Phytologist* **73**: 731–741.

Sun K, Zhang F-M, Kang N, Gong J-H, Zhang W, Chen Y, Dai C-C. **2019**. Rice carbohydrate dynamics regulate endophytic colonization of Diaporthe liquidambaris in response to external nitrogen. *Fungal Ecology* **39**: 213–224.

Tanney JB, Seifert KA. **2020**. Mollisiaceae: An overlooked lineage of diverse endophytes. *Studies in Mycology* **95**: 293–380.

Tellenbach C, Grünig CR, Sieber TN. **2011**. Negative effects on survival and performance of Norway spruce seedlings colonized by dark septate root endophytes are primarily isolate-dependent. *Environmental Microbiology* **13**: 2508–2517.

U'Ren JM, Lutzoni F, Miadlikowska J, Zimmerman NB, Carbone I, May G, Arnold AE. **2019**. Host availability drives distributions of fungal endophytes in the imperilled boreal realm. *Nature Ecology & Evolution* **3**: 1430–1437.

Vandenkoornhuyse P, Quaiser A, Duhamel M, Le Van A, Dufresne A. **2015**. The importance of the microbiome of the plant holobiont. *New Phytologist* **206**: 1196–1206.

Via S. **1984**. The Quantitative Genetics of Polyphagy in an Insect Herbivore. II. Genetic Correlations in Larval Performance Within and Among Host Plants. *Evolution* **38**: 896–905.

Wagner A. **2011**. Genotype networks shed light on evolutionary constraints. *Trends in Ecology & Evolution* **26**: 577–584.

Westrick NM, Smith DL, Kabbage M. **2021**. Disarming the Host: Detoxification of Plant Defense Compounds During Fungal Necrotrophy. *Frontiers in Plant Science* **12**.

Wisecaver JH, Slot JC, Rokas A. **2014**. The Evolution of Fungal Metabolic Pathways. *PLOS Genetics* **10**: e1004816.

Yang H, Zhao X, Liu C, Bai L, Zhao M, Li L. **2018**. Diversity and characteristics of colonization of root-associated fungi of Vaccinium uliginosum. *Scientific Reports* **8**: 15283.

Zanne AE, Abarenkov K, Afkhami ME, Aguilar-Trigueros CA, Bates S, Bhatnagar JM, Busby PE, Christian N, Cornwell WK, Crowther TW, *et al.*2020. Fungal functional ecology: bringing a trait-based approach to plant-associated fungi. *Biological Reviews* **95**: 409–433.

Figure legends

Figure 1: A conceptual overview of this study.

Figure 2: Two lineages of Mollisiacean endophytes sampled from wild *Vaccinium angustifolium* roots across multiple sites in Eastern North America. A) A maximum likelihood phylogeny of the ITS sequences of all Mollisiacean fungi isolated as part of this study and reference sequences obtained from public databases. Isolates from this study are highlighted in green if part of the *Phialocephala fortinii* s.l. – *Acephala applanata* species complex (PAC), highlighted in orange if part of the ad-hoc phylogenetic group Clade D, and reference sequences are not highlighted. Bootstrap support is labeled in red and all branches with <70% bootstrap support have been collapsed. B) Pictures of typical Clade D (left) and PAC (right) isolates after two weeks growth on 1% blueberry root extract media C) Approximate locations of sample sites in Pennsylvania (PA) and Virginia (VA), with the proportion of each lineage from each site visualized as a pie chart.

Figure 3: Endophyte lineages differ in their intrinsic growth rates and respond differently to specific plant metabolites, metabolite classes, and plant tissue extracts. Dot plots displaying fungal growth (cm^2 x 7 days), as measured by the Area Under the Growth Progress Stairs (AUGPS), in response to A) metabolite treatments, B) metabolite class and C) plant tissue extracts. Least-squared means were calculated separately for the PAC and Clade D lineages and are overlaid as a large circle on top of individual data points that represent all cohorts and replicates of each isolate for each treatment. Individual data points are color coded by lineage, while treatment means that differ significantly from the control (panel A; $\boldsymbol{\alpha} = 0.05$) or from the blueberry root tissue extract treatment (panel C; $\boldsymbol{\alpha} = 0.05$) are color coded by lineage and otherwise have a white fill if not significant. Error bars represent the 95% confidence interval, and points are arranged to be non-overlapping with jitter = 0.02.

Figure 4: Metabolic trait architecture is largely conserved between endophyte lineages. Top: scaled biplots where the X and Y axes represent the first two principal components of the phenotypic variance/covariance (**P**) matrix for metabolic traits in each of the two endophyte

lineages for A) the metabolite experiment and B) the tissue experiment. Individual points represent individual isolates. Loadings for individual metabolites or host tissues along PC1/P_{max} and PC2 are drawn as black arrows and labeled in red. Bottom: Null distributions and observed values for the three matrix comparison statistics (difference in total phenotypic variance, difference in percent variance along PC1/P_{max} and difference in the orientation of PC1/P_{max}) for C) the metabolite experiment and D) the tissue experiment. Null distributions were calculated by permuting isolates among lineages and comparing the features of 500 randomly permuted matrix pairs.

Figure 5: The vast majority of pairwise metabolic trait correlations do not differ between endophyte lineages. Each cell in these two matrices contains a *P* value associated with the null hypothesis that the pairwise trait correlation does not differ between the PAC and Clade D lineages for A) metabolite experiment and B) tissue experiment. Statistical comparisons of Spearman's rank correlation coefficients were conducted using the Fisher's *z* test.

Supporting Information Legends

Figure S1: The linear association between carbon concentration and growth across all metabolite treatments and fungal lineages

Figure S2: Spearman's rho correlations between growth across a) metabolite treatments and b) tissue extract treatments for the PAC and Clade D fungal lineages. Non-significant correlations ($P > 0.05$) are crossed out.

Table S1: Fungal isolate ITS genotyping and best BLASTn hit from NCBI nr

Table S2: Carbohydrate and Phenolic metabolites known to be produced by Vaccinium species

Table S3: Metabolite treatments with no statistically discernible effect on the growth of either PAC or Clade D lineages

Table S4: Least squared means comparisons of all treatments vs. ethanol control in PAC and cladeD

Table S5: Least squared means comparisons between PAC and cladeD for each metabolite treatment

Table S6: Least squared means comparisons between PAC and cladeD for carbohydrates and phenolics

Table S7: Anova of fixed effects in model for phenolics vs carbohydrates, excluding caffeic acid

Table S8: Least squared means comparisons between PAC and cladeD for carbohydrates and phenolics, excluding caffeic acid

Table S9: Least squared means comparisons of all tissue extract treatments in PAC and cladeD

Table S10: Tests for differences between the pairwise trait correlations of cladeD and PAC for both the metabolite and tissue experiment

A) Metabolic trait phenotyping

Plant metabolite experiment

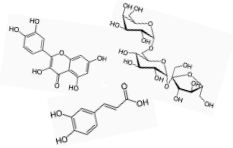

Measure growth on 11 plant metabolites in host root extract

Plant tissue experiment

Measure growth on 5 plant tissue extracts

B) Questions and approach

1. Do lineages differ in their mean response to individual plant substrates?

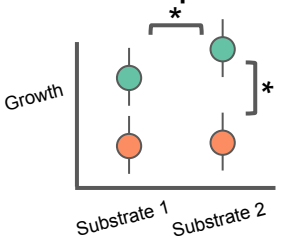

Comparison of trait means

Endophyte lineages: Clade D PAC

2. Do lineages differ in their multivariate metabolic trait architectures?

Difference in the total amount of trait variance (P matrix volume)

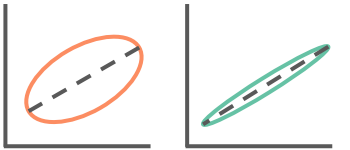

Difference in the strength of trait covariation (proportion of variation along P_{max})

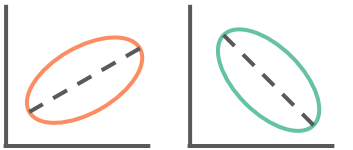

Difference in the orientation of trait covariation (angle between P_{max})

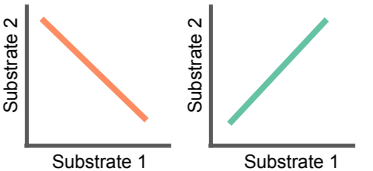

Comparison of pairwise trait correlations

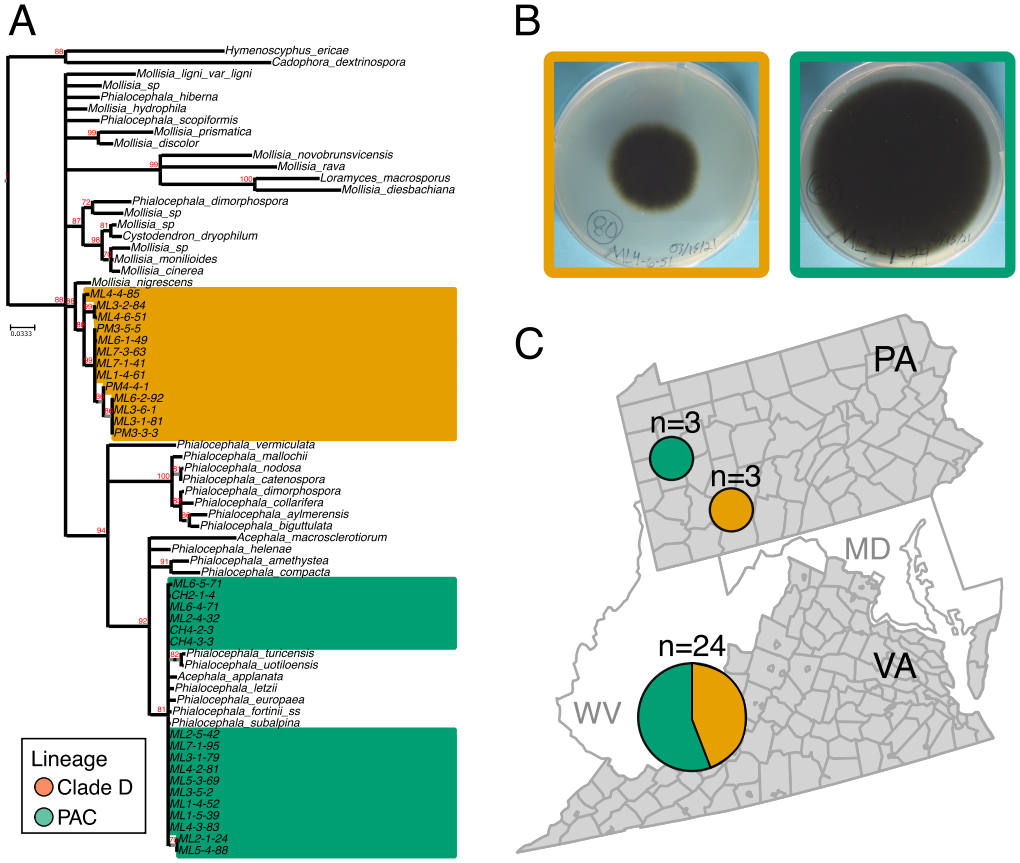
A
Hymenoscyphus_ericae
Cadophora_dextrinospora
Mollisia_ligni_var_ligni
Mollisia_sp
Phialocephala_hiberna
Mollisia_hydrophila
Phialocephala_scopiformis
Mollisia_prismatica
Mollisia_discolor
Mollisia_novobrunsvicensis
Mollisia_rava
Loramyces_macrosporus
Mollisia_diesbachiana
Phialocephala_dimorphospora
Mollisia_sp
Mollisia_sp
Cystodendron_dryophilum
Mollisia_sp
Mollisia_monilioides
Mollisia_cinerea
Mollisia_nigrescens
ML4-4-85
ML3-2-84
ML4-6-51
PM3-5-5
ML6-1-49
ML7-3-63
ML7-1-41
ML1-4-61
PM4-4-1
ML6-2-92
ML3-6-1
ML3-1-81
PM3-3-3
Phialocephala_vermiculata
Phialocephala_mallochii
Phialocephala_nodosa
Phialocephala_catenospora
Phialocephala_dimorphospora
Phialocephala_collariferа
Phialocephala_aylmerensis
Phialocephala_biguttulata
Acephala_macrosclerotiorum
Phialocephala_helenae
Phialocephala_amethystea
Phialocephala_compacta
ML6-5-71
CH2-1-4
ML6-4-71
ML2-4-32
CH4-2-3
CH4-3-3
Phialocephala_turicensis
Phialocephala_uotiloensis
Acephala_applanata
Phialocephala_letzii
Phialocephala_europaea
Phialocephala_fortinii_ss
Phialocephala_subalpina
ML2-5-42
ML7-1-95
ML3-1-79
ML4-2-81
ML5-3-69
ML3-5-2
ML1-4-52
ML1-5-39
ML4-3-83
ML2-1-24
ML5-4-88
0.0333
Lineage
Clade D
PAC
B
C
PA
n=3
n=3
MD
n=24
VA
WV

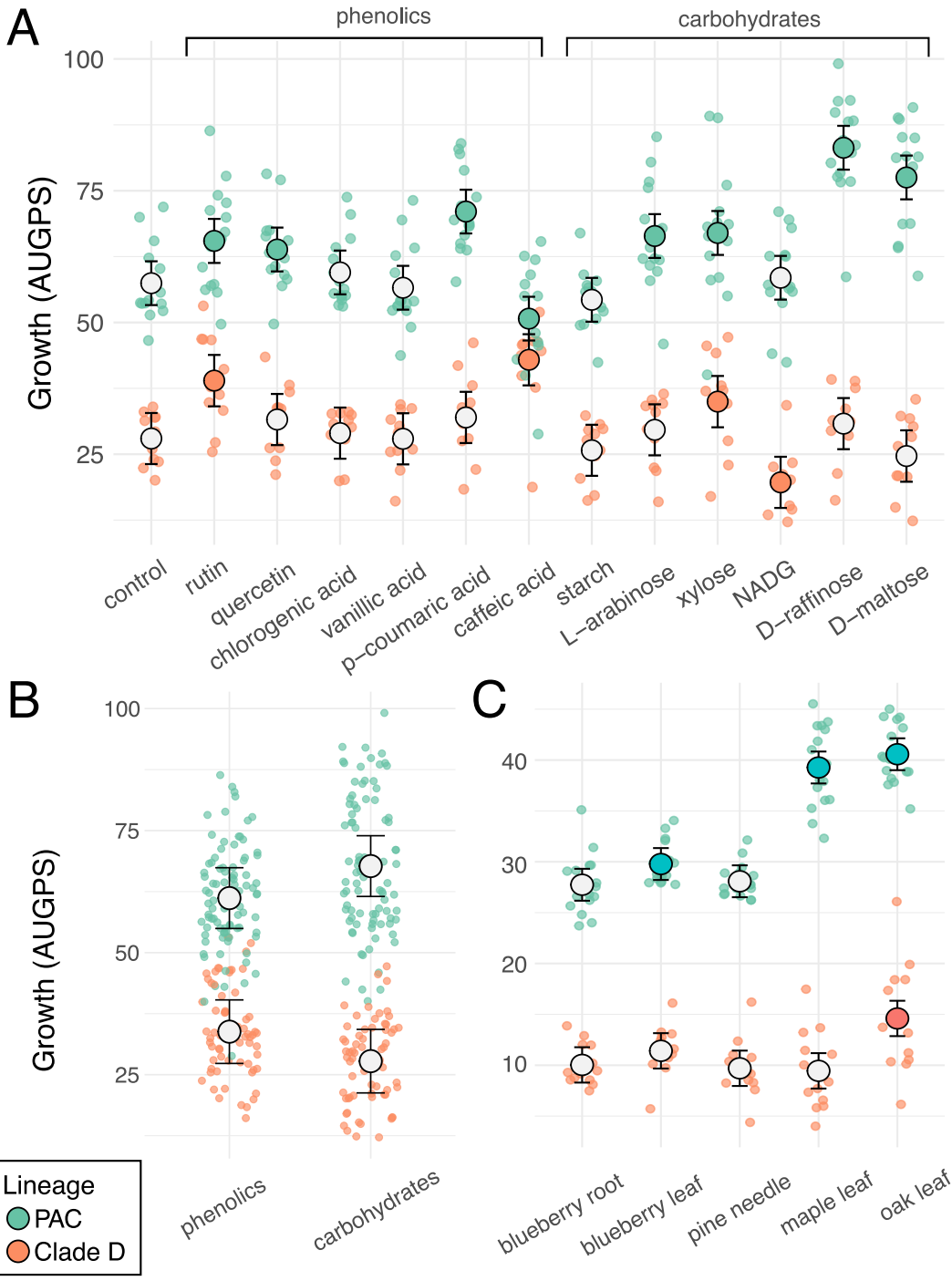
A
phenolics
carbohydrates
Growth (AUGPS)
100
75
50
25
control
rutin
quercetin
chlorogenic acid
vanillic acid
p−coumaric acid
caffeic acid
starch
L−arabinose
xylose
NADG
D−raffinose
D−maltose
B
Growth (AUGPS)
100
75
50
25
phenolics
carbohydrates
C
40
30
20
10
blueberry root
blueberry leaf
pine needle
maple leaf
oak leaf
Lineage
PAC
Clade D

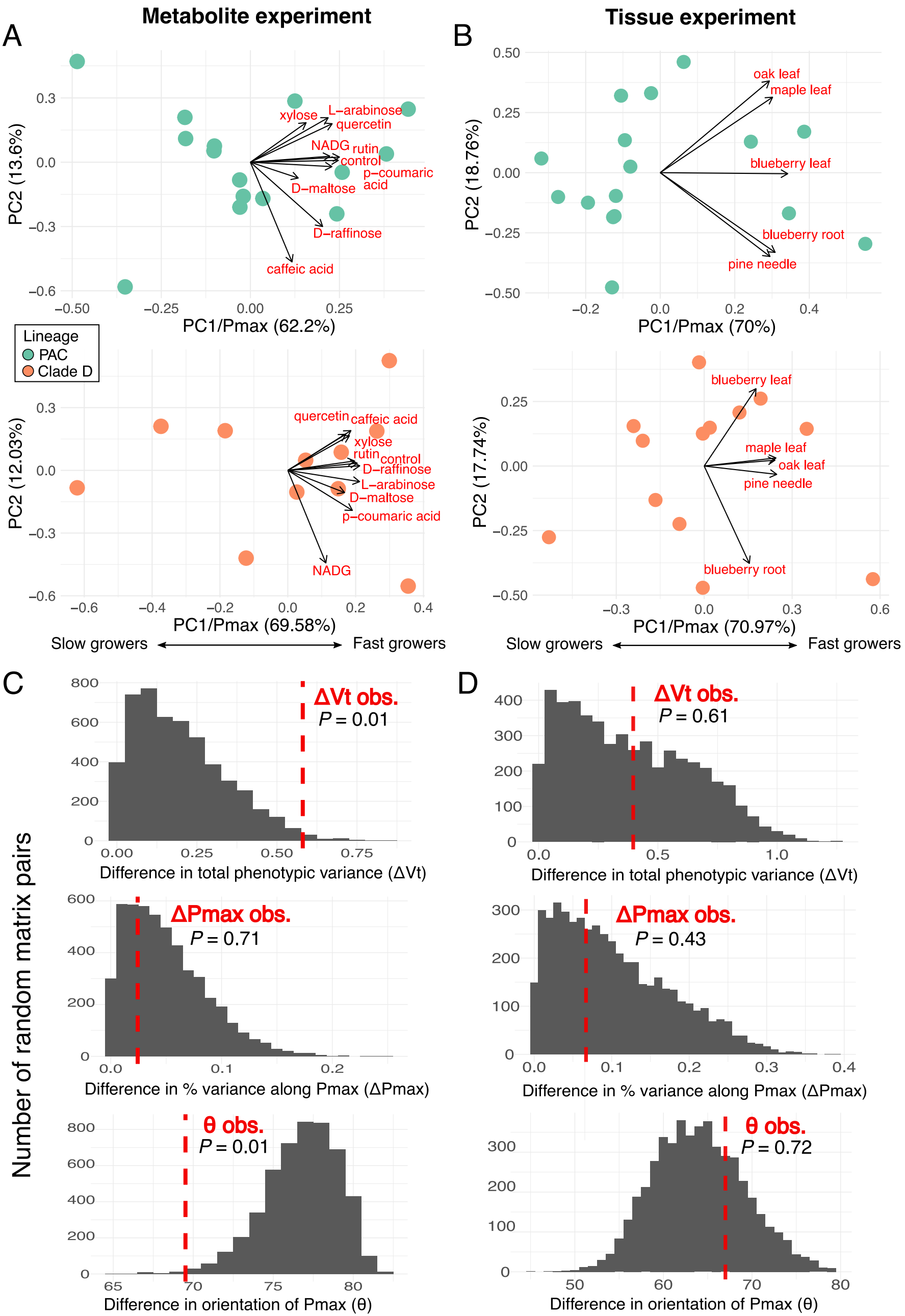
Metabolite experiment
Tissue experiment
A
B
C
D
PC2 (13.6%)
PC1/Pmax (62.2%)
xylose
L−arabinose
quercetin
NADG
rutin
control
p−coumaric acid
D−maltose
D−raffinose
caffeic acid
PC2 (18.76%)
PC1/Pmax (70%)
oak leaf
maple leaf
blueberry leaf
blueberry root
pine needle
Lineage
PAC
Clade D
PC2 (12.03%)
PC1/Pmax (69.58%)
quercetin
caffeic acid
xylose
rutin
control
D−raffinose
L−arabinose
D−maltose
p−coumaric acid
NADG
PC2 (17.74%)
PC1/Pmax (70.97%)
blueberry leaf
maple leaf
oak leaf
pine needle
blueberry root
Slow growers
Fast growers
Number of random matrix pairs
ΔVt obs.
P = 0.01
Difference in total phenotypic variance (ΔVt)
ΔVt obs.
P = 0.61
Difference in total phenotypic variance (ΔVt)
ΔPmax obs.
P = 0.71
Difference in % variance along Pmax (ΔPmax)
ΔPmax obs.
P = 0.43
Difference in % variance along Pmax (ΔPmax)
θ obs.
P = 0.01
Difference in orientation of Pmax (θ)
θ obs.
P = 0.72
Difference in orientation of Pmax (θ)

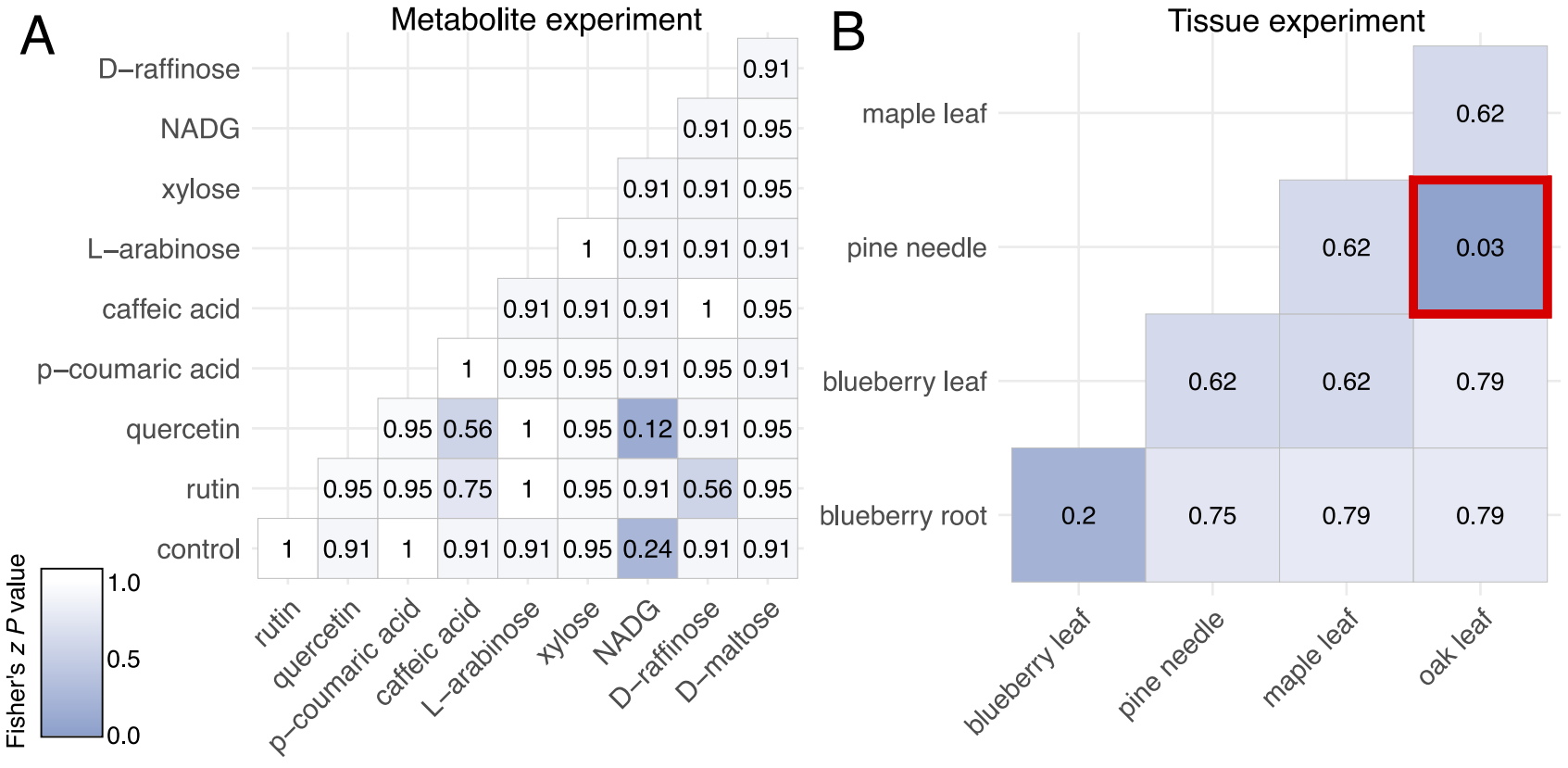
A
Metabolite experiment
D−raffinose
NADG
xylose
L−arabinose
caffeic acid
p−coumaric acid
quercetin
rutin
control
rutin
quercetin
p−coumaric acid
caffeic acid
L−arabinose
xylose
NADG
D−raffinose
D−maltose
Fisher's z P value
1.0
0.5
0.0
B
Tissue experiment
maple leaf
pine needle
blueberry leaf
blueberry root
blueberry leaf
pine needle
maple leaf
oak leaf